Date of revision: 30/10/2025

An analysis of aggregate crumb rubber mixture packing

Author 1
Rafael Anjos, MSc
CERIS, Department of Civil Engineering, University of Aveiro, Portugal
0009-0001-4839-9343
rafaelanjos@ua.pt
Author 2
Margarida Pinho-Lopes, PhD
CERIS, Department of Civil Engineering, University of Aveiro, Portugal
0000-0003-0808-6307
mlopes@ua.pt
Author 3
William Powrie, CBE FREng MA MSc PhD CEng FICE FPWI
Faculty of Engineering and Physical Sciences, University of Southampton, United Kingdom
0000-0002-2271-0826
W.Powrie@soton.ac.uk

Corresponding author e-mail: rafaelanjos@ua.pt

Number of words in the main text:

Abstract (150 – 200 words)

Ballasted track has provided a cost-effective support for railway infrastructure. Modern trains, generate high loads increasing ballast degradation. The inclusion of crumb rubber has been proposed as a mitigation measure. Typically, the optimal crumb rubber content suggested in the literature is 10%, sometimes by weight and sometimes by volume. These represent significantly different material contents: 10% by weight is nearly double 10% by volume. This study investigates the packing of $^1/_3$-scale ballast intermixed with two crumb rubber sizes at 10% by weight and by volume of aggregate particles. The analysis considers both a traditional two-phase framework, in which crumb rubber is considered part of particulate skeleton, and a novel three-phase framework, where crumb rubber is considered as a separate phase from aggregate particles and voids. The two-phase framework showed reduced maximum and minimum void ratios when crumb rubber was mixed with scaled ballast. The three-phase framework, however, indicated increased intergranular void ratios, suggesting that crumb rubber disrupts aggregate packing or an effective crumb rubber content different from the target value. Observations from transparent box tests revealed segregation and stratification of rubber particles within the matrix. The results highlight the need for further study of mixing methods and segregation mechanisms.

Keywords chosen from ICE Publishing list

Ground improvement, Railway track, Waste valorisation, Mathematical modelling

List of notations (examples below)

U *Uniformity coefficient* = D_{60}/D_{10}

CR *Crumb rubber*

CR_c *Crumb rubber content by total weight of particles*

$CR_{c,th}$ *Crumb rubber content threshold by total weight of particles*

CS_{50} *Coarse spheres effective mean size*

D_{max} *Maximum particle size*

D_n *Effective mean diameter for n% passing*

e *Void ratio*

e_a *Void ratio of aggregate on its own*

e_{cr} *void ratio of crumb rubber on its own*

e_{global} *Global void ratio*

$e_{global,max}$ *Maximum global void ratio*

$e_{global,min}$ *Minimum global void ratio*

$e_{intergran}$ *Intergranular void ratio*

$e_{intergran,\ max}$ *Maximum intergranular void ratio*

$e_{intergram,\ min}$ *Minimum intergranular void ratio*

e_{max} *Maximum void ratio*

e_{min} *Minimum void ratio*

G_a *Aggregate grain specific gravity*

$G_{a,cr}$ *Aggregate / crumb rubber mixtures (M) grain specific gravity*

G_{cr} *Crumb rubber grain specific gravity*

V_{cr}/V_a *Percentage of crumb rubber, relative to aggregate grains, by volume*

W_{cr}/W_a *Percentage of crumb rubber, relative to aggregate grains, by weight*

R_D *Size disparity ratio =* CS_{50}/SS_{50}

SS_{50} *Small spheres effective mean size*

SD Standard deviation

V_g *Volume of solid particles (aggregate + crumb rubber)*

$V_{s,a}$ *Volume of solid aggregate*

$V_{s,cr}$ *Volume of solid crumb rubber*

V_v *Volume of voids*

$V_{v,t}$ *Volume of total voids*

$V_{v,a}$ *Volume of voids associated with the aggregate*

$V_{v,cr}$ *Volume of voids associated with the crumb rubber*

γ_a *Aggregate bulk unit weight*

γ_{cr} *Crumb rubber bulk unit weight*

γ_{max} *Maximum bulk unit weight*

γ_{min} *Minimum bulk unit weight*

τ *Shear stress*

δ *Shear strain*

$\%_{cr,\,T}$ *Percentage of added crumb rubber by total weight (aggregate plus crumb rubber particles)*

$\%_{cr,\,A}$ *Percentage of added crumb rubber by weight of aggregate particles*

1 Introduction

Ballasted railway track has a long history of excellent performance. However, with increasing number of train passages, railway track settles differentially along its length. To reinstate track geometry and ensure that trains run safely, maintenance is required. Maintenance constitutes a significant percentage of annual railway operational costs (Esmaeili *et al.,* 2020; Rempelos *et al.*, 2020).

Furthermore, trains are becoming faster and carrying heavier loads, and railway lines are experiencing a growth in traffic intensity. Hence, in the future, railway track will need to withstand higher loads, imposed by faster and heavier trains, with reduced time available to carry out maintenance and renewal works. In this light, the increasing popularity of ballastless track designs, such as slab track, is not surprising (Esveld, 2023). However, high up-front costs, the need for precision in construction and the narrow range of post-installation adjustment that can be made to correct track settlements, make slab track viable only for heavily trafficked lines.

Various proposals have been made for improving the performance of ballasted railway track. These include polyurethane (Kennedy *et al.*, 2013) or cement impregnation (Le *et al.*, 2020), bitumen underlay (D'Angelo *et al.*, 2016), geosynthetic inclusions (Brown *et al.*, 2007) and crumb rubber intermixed with ballast (Guo *et al.,* 2019). Crumb rubber is sourced from end-of-life road vehicles tires. According to Indraratna (2023), the soft and elastic nature of rubber can potentially reduce the aggressiveness of inter-particle contacts, minimizing the need for annual maintenance by about 40%.

Studies based on large scale triaxial, impact load and ballast box tests have suggested that the amount of crumb rubber that needs to be mixed with the ballast to reduce ballast grain breakage without significantly affecting the bulk stiffness is about 10%. However, some researchers have proposed 10% by total weight (Arachchige *et al.*, 2021, 2022), and others 10% by total volume (Sol-Sánchez *et al.*, 2015; Esmaeili *et al.*, 2016; Koohmishi and Azarhoosh, 2021). Furthermore,

there is only limited understanding of how crumb rubber and ballast particles mix and interact. For railway engineering applications, it is important to be able to identify features such as stratification, inhomogeneities and voids, which will affect the mechanical behaviour of mixtures (Edil, 1988; Thevanayagam *et al.*, *2002*; Tasalloti *et al.*, 2021).

Like a soil, railway ballast is a multiphase material comprising solid (discrete particles), gas (usually air) and liquid (usually water) phases. Interparticle spaces are known as voids, and aggregate grains are reasonably free to rearrange to form a load-bearing matrix. The arrangement of particles within an aggregate element is termed the packing, usually quantified by means of the void ratio (e), i.e., the ratio of the volume of voids (V_v) to the volume of solid grains (V_g). The densest packing possible corresponds to the minimum void ratio, e_{min}, and the loosest to the maximum void ratio, e_{max}.

Traditionally, crumb rubber intermixed with ballast has been studied as a two-phase material (solid particles and air), i.e., with the crumb rubber particles considered part of the aggregate skeleton. Arachchige *et al.* (2022) used Equation 1 to represent the average aggregate crumb rubber mixture specific gravity, $G_{a,cr}$, as a function of G_a and G_{cr}, which are the aggregate and the crumb rubber specific gravity, respectively, and $\%_{cr,T}$ – the percentage of crumb rubber by total weight of (aggregate plus crumb rubber) particles.

$$G_{a,cr}=\frac{1}{\left(\frac{1-\%_{cr,T}}{G_a}\right)+\frac{\%_{cr,T}}{G_{cr}}} \quad (1a)$$

If $\%_{cr,A}$ is the ratio of the weight of crumb rubber particles to the weight of aggregate (stone) particles only, Equation (1a) becomes

$$G_{a,cr}=\frac{1+\%_{cr,A}}{\left(\frac{1}{G_a}\right)+\frac{\%_{cr,A}}{G_{cr}}} \quad (1b)$$

Exposure of granular mixtures to loading and vibration may result in particle segregation according to size (Rosato *et al.*, 1987; Makse *et al.*, 1997; Kudrolli, 2004). Large and dense

particles normally rise to the top, while small and light particles tend to fall to the bottom. However, if contact forces between particles are eliminated, dense particles may sink. For example, when a non-uniform aggregate is poured into a heap, large particles are more likely to be found near the base, and the small particles near the top. If the larger particles have a higher angle of repose than the smaller particles, segregation followed by stratification may occur on pouring, with the stratification not influenced by differences in particle density (Makse *et al.*, 1997).

Thus, crumb rubber intermixed with ballast may segregate and stratify when poured onto railway track, as illustrated by Makse *et al.* (1997) for sands. Crumb rubber particles may also then segregate during service loading, reducing or even eliminating their potential benefit in reducing maintenance costs. Lee *et al.* (2007) observed that in sand and rubber mixtures, and depending on rubber content, different force chains are formed, leading to the development of both rigid and soft granular skeletons. Further investigation into segregation and stratification is needed to better understand their implications for the in-service behaviour of crumb rubber intermixed with ballast in large-scale applications.

This paper reports the results of an experimental study carried out to investigate the influence of crumb rubber size on aggregate packing, using two wooden boxes – one fully opaque and the other with two transparent faces. Two different crumb rubber contents – 10% of the aggregate (stone) particles by volume and 10% of the aggregate particles by weight - were considered for two different crumb rubber particle sizes. Specimens were compacted using a shaking table. The mixture packing structure and the distribution of crumb rubber within the aggregate were analysed both quantitatively and qualitatively, to determine whether segregation and / or stratification occurred. In contrast to the traditional analysis in which both crumb rubber and aggregates are considered as solids, a framework to describe the packing of rubber-aggregate mixtures is proposed in which the crumb rubber is considered as a separate phase, distinct from both the voids and the aggregate solids.

2 Materials and methods

2.1 Aggregate

Freshly quarried gneiss granular aggregate was sourced from *Irmãos Cavaco* quarry (Aveiro, Portugal). The aggregate was chosen to obtain a particle size distribution corresponding to a $^1/_3$ scaling ($^1/_3$-scale ballast) of the full-scale ballast used on European railways, in accordance with BS EN 13450 (British Standards Institution, 2012).

The representativeness of tests on scaled-down granular aggregates to the full-scale has been widely debated. As reported by Delgado *et al.* (2019) and De Andrade *et al.* (2025), some researchers have observed an increase in strength of the scaled material (Leslie, 1963; Kirkpatrick, 1965), some a reduction (Dunn and Bora; 1972; Shenton, 1978), and others no significant difference where the properties of particle shape, roughness and strength are similar to those of the full-scale material (Vallerga *et al.*, 1956; Selig and Roner, 1987).
The issue was investigated in detail by Le Pen *et al.* (2013), who identified a weak trend for larger ballast grains to have a lower ratio of smallest to longest dimension (aspect ratio) and greater angularity than smaller grains, although comparison between any two individual sieve intervals may not follow these trends. However, the ranges of variation were small enough not to militate against the use of scaled materials as appropriate substitutes for testing purposes. In essence, the behaviour of a scaled railway ballast might be slightly different from that of the full-size material, but it still behaves essentially as “ballast”, especially as form and angularity are not normally closely specified in codes and standards. Certainly, scaled ballast testing can be used to gain insights into mechanisms of behaviour, as demonstrated by Sevi (2008) in general terms, and by Le Pen *et al.* (2014), Koike *et al.* (2014) and Xu *et al.* (2024) in the context of the static and earthquake resistance of railway sleepers and track to lateral movement.

In the research described in this paper, the particle shape, roughness and strength of the scaled ballast aggregates were not characterized. However, the material is from a quarry that supplies full-size ballast for railway use from the same parent rock, so within the caveats outlined by

Le Pen *et al.* (2013) regarding minor variations in grain aspect ratio and angularity, the scaled ballast used can be considered representative of this type of ballast in the round.

Figure 1 shows the particle size distribution of the aggregate and some of its physical properties, such including the effective diameter for 50% passing, D_{50}, and the uniformity coefficient, U. The grain specific gravity of the ballast particles, G_s, was 2.5. The effective friction angle of the 1/3-scale ballast was determined as 39°, with a standard deviation (SD) = 0.36, by pouring three specimens of the material, each of mass 7.38 kg, onto a flat surface and measuring the resulting angle of repose. The effective friction angle determined in this way is likely to correspond to that at the critical state. Similar effective friction angles have been reported for other coarse granular aggregates in monotonic triaxial tests (for example Ajayi, 2014; Gupta, 2023). Higher friction angles have also been reported (for example Suiker *et al.*, 2005; Indraratna *et al.*, 2006; Aingaran, 2014). However, these correspond to peak states, with dilation at or close to its maximum.

2.2 Crumb rubber

The crumb rubber studied was provided by *Genan* (Aveiro, Portugal). Two particle size ranges were used; a finer range (CR 0.8/3), with particles between 0.8 mm and 3.0 mm in diameter, and a coarser range (CR 3/7), with particles between 3.0 mm and 7.0 mm. Particle size distributions and some physical properties are shown in Figure 1. The finer crumb rubber, CR 0.8/3, was chosen to investigate how small elastic particles might ravel through a coarse rigid skeleton. The coarser crumb rubber, CR 3/7, is approximately 1/3 the size of the crumb rubber used by Sol-Sánchez *et al.* (2015) and Arachchige *et al.* (2021, 2022) in tests on full-scale ballast. The grain specific gravity of the crumb rubber was 1.2 for both fine and coarse material, assessed using the method described in BS EN 1097-6 (British Standards Institution, 2022). The effective friction angle of the crumb rubber was determined using a similar procedure to that for the 1/3-scale ballast. The angle of repose obtained was on average 15º (SD = 2.62) for CR 0.8/3 and 19º (SD = 1.00) for CR3/7.

142 The minimum and maximum void ratios of the crumb rubber were determined by filling a
143 graduated cylinder with a known mass of the material and measuring its total volume, testing
144 four specimens per condition. To obtain the loosest state, crumb rubber was placed gently into
145 the cylinder. To obtain the densest state, crumb rubber was subjected to multidirectional
146 vibration (frequency 50 Hz and amplitude 2.0 mm for 30 s). Ahmed and Lovell (1993) used a
147 vertically vibrating table and reported that vibratory compaction might not be appropriate for
148 pure granulated rubber. In this study, $^1/_3$-scale ballast and mixtures of $^1/_3$-scale ballast and
149 crumb rubber were compacted using vibration, so that the methods used to characterise
150 packing were the same. The minimum void ratios obtained were 1.34 (SD = 0.04) and 1.11
151 (SD = 0.10) for CR 0.8/3 and CR 3/7, respectively. The maximum void ratios obtained were 1.83
152 (SD = 0.03) and 1.48 (SD = 0.02) for CR 0.8/3 and CR 3/7, respectively. Void ratios around and
153 greater than 1 were also reported by Tasalloti *et al.* (2021) for crumb rubber.
154
155 The stress-strain behaviour of the crumb rubber was evaluated through direct shear tests in a
156 60×60 mm$^2 \times 12.5$ mm high shear box. All specimens were tested dry at four different vertical
157 stress values, at a shear rate of 1 mm/min. All specimens were prepared in a similar way. A
158 predetermined mass of crumb rubber (53 g for CR 0.8/3 and 47 g for CR 3/7) was carefully
159 placed into the shear box with 0 mm of free fall, to obtain the loosest possible initial condition.
160 The density of each specimen at the start of shear was determined taking into account the
161 measured vertical movement of the box top plate when the vertical stress was first applied.
162 Analogous compaction indices were difficult to obtain, as crumb rubber is highly compressible.
163

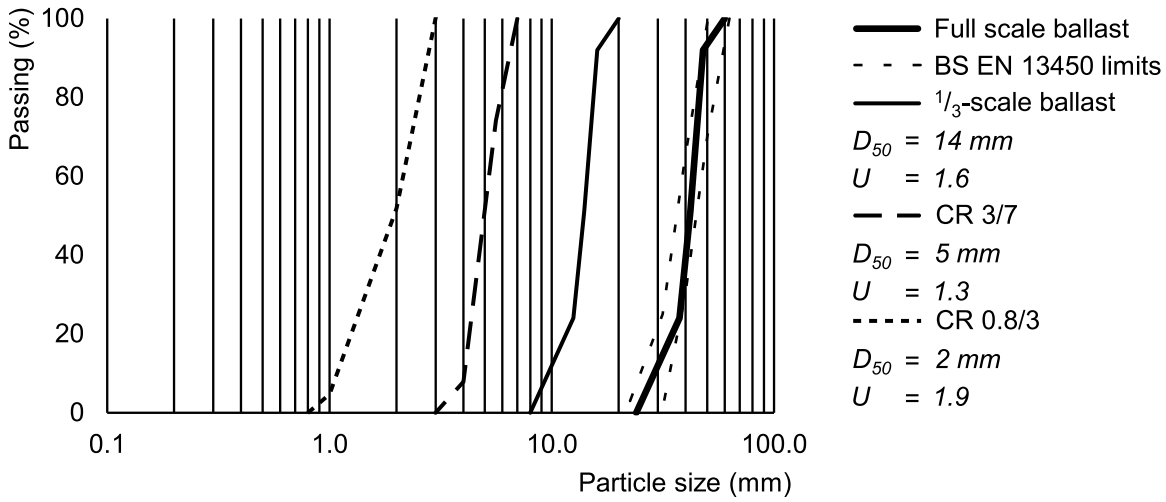

Figure 1. Particle size distribution of the $^1/_3$-scale ballast, the corresponding full-scale ballast (within the BS EN 13450 limits) and the two crumb rubber ranges (CR 0.8/3 and CR 3/7).

2.3 Packing tests

The influence of adding crumb rubber on the packing of $^1/_3$-scale ballast was studied in packing tests. Quantification using the traditional two-phase framework, with crumb rubber particles considered to be part of overall granular skeleton, was compared to a three-phase framework in which the crumb rubber was considered neither as part of the aggregate nor as part of the voids, but as a material in its own right.

Packing tests were carried out in two plywood boxes. Box 1 was a cubic container with an internal dimension of 300 mm and all faces made of 16 mm-thick plywood. Box 2 was a rectangular parallelepiped container with two 8 mm thick plexiglass windows to allow visual inspection. Its internal plan dimensions were 300 mm along the plane of the plexiglass window and 268 mm in the perpendicular direction; its internal height was 300 mm. The influence of the box dimensions on the aggregate behaviour was neglected as the internal edges of the boxes (300 and 268 mm) were significantly greater than six times the maximum particle size, D_{max} (Lade, 2016). Box 1 was used for the quantitative tests, and Box 2 for visual inspection of the packing.

A cement mixer, operating at a low rotational speed (24 revolutions per minute), was used to mix crumb rubber with $^1/_3$ scale-ballast for approximately 60 seconds. This method, used by Arachchige *et al.* (2022), is a rapid and simple way of mixing a considerable amount of material (50 kg of $^1/_3$-scale ballast per specimen), with minimal particle breakage.

Packing tests were carried out to characterise the loosest and densest stable states for the natural $^1/_3$-scale ballast and four different mixtures of $^1/_3$-scale ballast with crumb rubber. In all tests, Box 1 was filled manually, taking $^1/_3$-scale ballast intermixed with crumb rubber from the cement mixer, and the mass and volume of the material placed in the test box were recorded. To obtain the loosest state, material was carefully placed in the box by hand, with no compaction, until the box was full and the final surface was levelled by adding and removing individual particles by hand. To obtain the densest state, the method described by Ferro *et al.* (2024) was adopted to avoid undue aggregate abrasion and breakage. The box was placed on a concrete shaking table and filled in three layers. After placing the first 100 mm thick layer, the box was subjected to shaking (50 Hz frequency, 0.8 mm amplitude for 300 s); this process was repeated for the second and third layers. The final layer was often slightly proud of the top of the box; to level the surface, the box lid was pressed manually against the aggregate. Once levelled, the lid was placed on the top of the box and the specimen height was measured using a calliper.

The percentage of crumb rubber by volume (V_{cr}/V_a) is related to the percentage of crumb rubber by weight (W_{cr}/W_a) by Equation 2, where G_a and G_{cr} are respectively the grain specific gravities of the aggregate and the crumb rubber. For the materials studied, the percentage of crumb rubber by weight, (W_{cr}/W_a), is approximately 47% of the percentage of crumb rubber by, volume, (V_{cr}/V_a), meaning that (V_{cr}/V_a) is nearly twice (W_{cr}/W_a).

$$\frac{W_{cr}}{W_a} = \frac{G_{cr}}{G_a} \times \frac{V_{cr}}{V_a} \qquad (2)$$

The packing tests using Box 1 were carried out on $^1/_3$-scale ballast and $^1/_3$-scale ballast intermixed with 10% of crumb rubber (CR 0.8/3 and CR 3/7) by weight (W_{cr}/W_a=10%) and by volume (V_{cr}/V_a=10%) of the aggregate particles. For each mixture, six packing tests were carried out; three for the loosest (e_{max}) and three for the densest (e_{min}) state, giving a total of 30 tests. Additionally, one packing test per condition was carried out in Box 2, resulting in five further tests.

2.4 Mixture fabric

Mixing crumb rubber within an aggregate might cause the aggregate packing to change. Figure 2 illustrates different possible packing scenarios, for a simplified case where all particles are incompressible spheres. Consider first the case of crumb rubber particles being introduced into a pre-existing aggregate matrix. If the crumb rubber particles are small relative to the aggregate voids, they will initially fill the voids without disrupting the packing of the aggregates (Figure 2a). This will continue up to a certain crumb rubber content threshold, $CR_{c,th}$ (Equation 3), at which the volume of crumb rubber solid particles, $V_{s,cr}$ and associated voids, $V_{v,cr}$, is equal to the volume of aggregate voids, $V_{v,a}$. In Equation 3, e_a is the void ratio of the aggregate and e_{cr} the void ratio of crumb rubber, each on its own.

$$CR_{c,th} = \frac{W_{cr}}{W_a} = \frac{G_{cr}}{G_a} \times \frac{e_a}{1+e_{cr}} \quad (3)$$

If the two materials are placed simultaneously, crumb rubber may separate the aggregate particles (Figure 2b), or a layered structure may develop (Figure 2c) (Makse *et al.*, 1997).

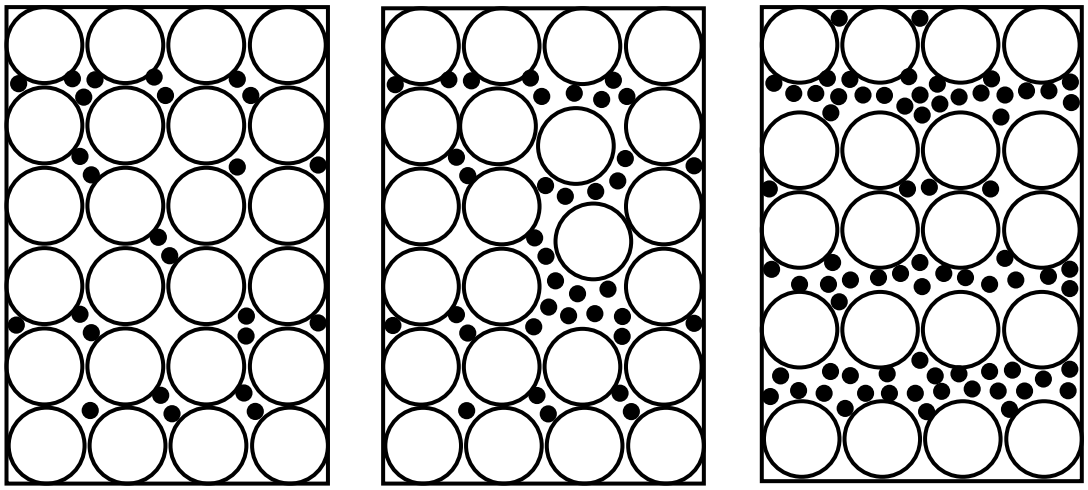

a) b) c)

Figure 2. Role of crumb rubber within aggregate packing for $CR_c < CR_{c,th}$ (simplified and incompressible particle shapes: spheres): a) Confined within aggregate particles [crumb rubber does not take part in the load path],b) Confined and partly in contact with aggregate particles [crumb rubber particles take some part in the load path], c) Layered [load path alternates through the aggregates and the crumb rubber with depth].

For real aggregates, with irregular particles shapes and distribution of sizes, packing deviates from the binary regular spheres represented in Figure 2. Nonetheless, consideration of an ideal binary system can offer some insights into the possible interference of crumb rubber particles with aggregate packing.

Single size spheres can arrange into five stable packings (Figure 3): simple cubic (e = 0.91), cubic-tetrahedral (e = 0.65), tetragonal sphenoidal (e = 0.43), pyramidal (e = 0.35) and tetrahedral (e = 0.35) (Mitchell *et al.*, 2025). Amongst these, simple cubic and cubic-tetrahedral exhibit interconnected voids (in the direction perpendicular to the plane of the paper), which smaller spheres mixed into the coarse skeleton may, if small enough, fill. The size disparity ratio (R_D), defined as the ratio of coarse sphere effective mean size (CS_{50}) to the small sphere effective mean size (SS_{50}), can be used as an analytical parameter to assess the voids penetration potential of a fine-coarse mixture (Thevanayagam *et al.*, 2002). With simple cubic packing, voids penetration may occur when $R_D > 2.4$ and with cubic-tetrahedral packing when $R_D > 6.5$. At lower values of R_D the particles are more similarly sized, the smaller grains cannot occupy the voids between the larger grains without disrupting their packing, and are more likely to form an undifferentiated mixed particulate matrix.

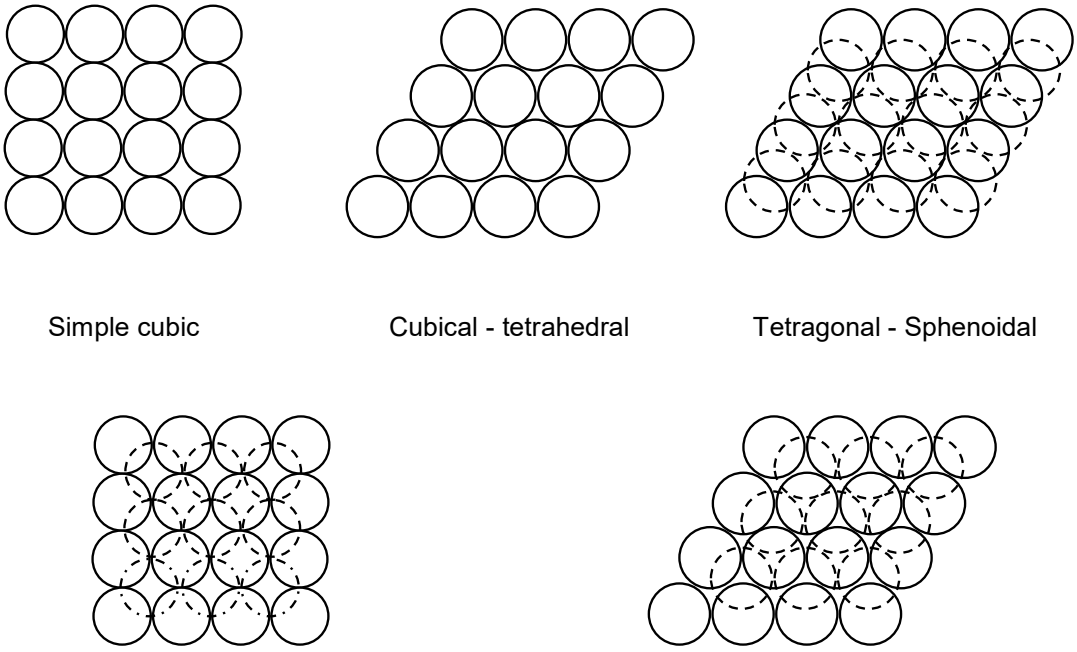

Figure 3. Assemblage of spheres in regular packing (adapted from Mitchell *et al.*, 2025).

When the crumb rubber content is below the relevant threshold, ($CR_c < CR_{c,th}$) and the size disparity ratio R_D is larger than 2.4 or 6.5 (depending on the aggregate packing), crumb rubber particles may be fully confined within aggregate particles (Figure 2a) or confined and partly in contact with aggregate particles (Figure 2b). If the crumb rubber is above the relevant threshold ($CR_c > CR_{c,th}$) or the size disparity ratio R_D is less than 2.4 or 6.5 (depending on the aggregate packing), the smaller grains will disrupt the packing of the larger.

For mixtures of two readily-identifiable particle types, two different void ratios can be defined: the intergranular void ratio, $e_{intergran}$ (Equation 4), and the mixture global void ratio e_{global} (Equation 5). In Equations 4 and 5, $V_{s,a}$ is the volume of aggregate (stone) solids particles, and $V_{v,t}$ is the total volume of voids of the mixture. In the intergranular void ratio, voids are comprised of all phases except the aggregate solid particles. In the global void ratio, the voids are the spaces between the solids (stone aggregate and crumb rubber); that is, both stone aggregates and crumb rubber grains are treated as solids.

$$e_{intergran} = \frac{V_{v,t} + V_{s,cr}}{V_{s,a}} \quad (4)$$

$$e_{global} = \frac{V_{v,t}}{V_{s,a} + V_{s,cr}} \quad (5)$$

If the crumb rubber particles are small enough to act as a filler within the aggregate skeleton, the intergranular void ratio, $e_{intergran}$, does not change until $CR_{c,th}$ is reached. However, the mixture global void ratio, e_{global}, diminishes as crumb rubber particles fill some of the aggregate natural voids.

By definition (Equation 3), the threshold crumb rubber content depends on the aggregate packing. When crumb rubber is incorporated into a loose packed aggregate, $CR_{c,th}$ is higher than for the aggregate in its dense state.

As the crumb rubber content is increased beyond the threshold value, some crumb rubber particles will start to interact with aggregate particles, disrupting their natural packing (Figure 2b). The intergranular void ratio of the mixture then starts to increase and the global void ratio to decrease. This model was developed true for soils and aggregates, whose particles are incompressible, but might not apply to compressible particles, which may deform rather than disrupt the surrounding incompressible particles. Hence considering elastic particles as a solid phase, and using only the global void ratio, e_{global}, to describe the mixture packing, may lead to an erroneous interpretation.

For layered packing (Figure 2c), the use of uniform intergranular and global void ratios to characterise the overall relation between solid particles and voids may not be suitable. For a stratified binary mixture, rubber layer deformation and the boundary between the two materials may have a greater influence on the overall structural behaviour than the interaction between the materials at the grain scale (Liang *et al.*, 2025).

3 Results and discussion

3.1 Frictional resistance of the crumb rubber

Figure 4 shows the stress-strain response of the crumb rubber (CR 0.8/3 and CR 3/7) tested on its own, under four different normal vertical stresses (27, 55, 109 and 164 kPa) in a 60×60 mm^2 $\times$ 12.5 mm high direct shear apparatus (shearbox). Continuous strain hardening was observed up to the maximum shear displacement (6 mm), no clear peak or asymptotic behaviour was observed. Similar behaviour was reported by Xiao *et al.* (2015) for tyre-derived aggregate with particles sizes ranging between 5 mm and 110 mm, tested in a large direct shear apparatus (790 × 800 mm^2 $\times$ 610 mm high).

At a shear strain of 20%, the mobilised effective friction angle was 39.8º for CR 0.8/3 and 38.7º for CR 3/7. These values are not a traditional strength, in the sense of being a limit state, as at the maximum shear strain, stress was still rising. Nonetheless, the observed friction angles are comparable with the values of 36.6º and 35.7º reported by Xiao *et al.* (2015) for larger particles (5 mm to 110 mm). The mobilised effective friction angles obtained from the direct shear tests were significantly greater than from the pouring technique (15º for CR 0.8/3 and 19º for CR 3/7), even recognising that the latter might have been affected by basal instability of the crumb rubber heap owing to the propensity of the crumb rubber particles to roll. In general, CR 0.8/3 exhibited a slightly higher mobilised effective friction angle than CR 3/7. When sheared, crumb rubber particles exhibit considerable compression and elastic deformation. This is quite different from the classical response of soils, in which the soil grains are assumed to be rigid and incompressible, and suggests that acceptable stress states for crumb rubber should be based on strain limits rather than strength. Further work is needed to fully understand crumb rubber mechanical behaviour in different modes of imposed deformation.

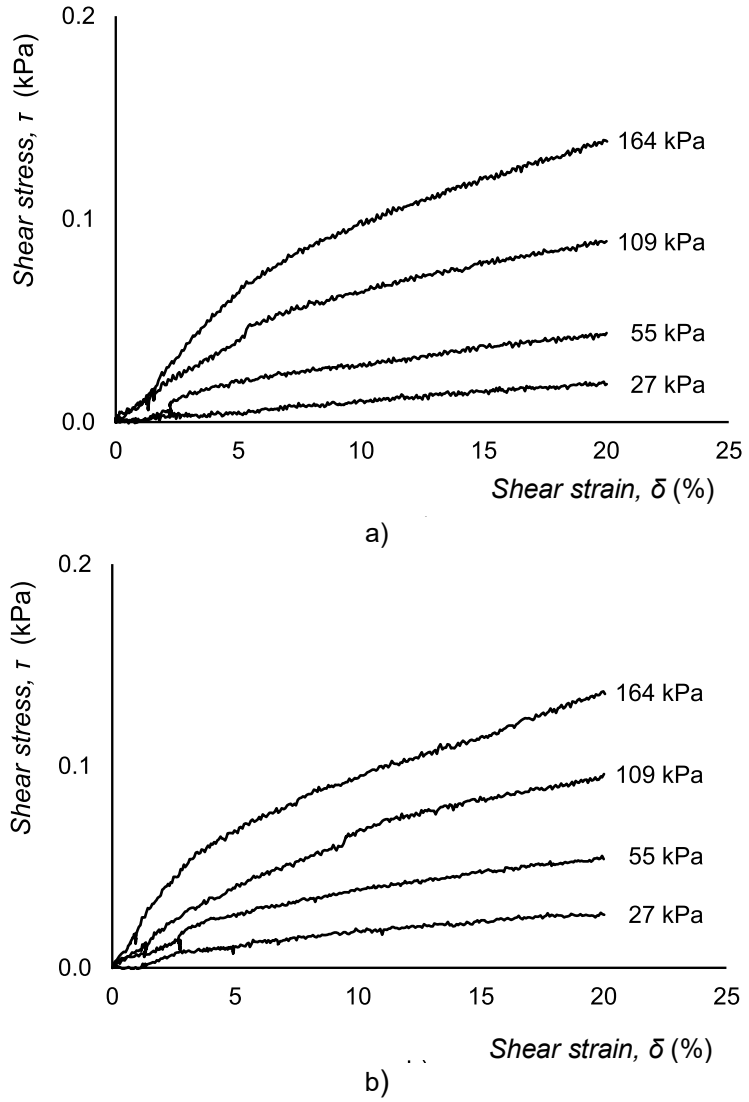

Figure 4. Crumb rubber direct shear test results (shear stress ,*τ,* plot against shear strain, *δ*) for different normal stresses a) CR 0.8/3 b) CR 3/7.

3.2 Influence of crumb rubber on the packing of $^1/_3$-scale ballast

Table 1 summarises the packing test results, including the crumb rubber content threshold, $CR_{c,th}$, size disparity ratio, R_D, minimum and maximum bulk unit weight, respectively γ_{min} and γ_{max}.

The finer crumb rubber tested, CR 0.8/3, was susceptible to segregation in both loose and dense conditions as its size disparity ratio, R_D, is greater than 6.5. The coarser crumb rubber studied, CR 3/7, might also be susceptible to segregation when mixed with loose $^1/_3$- scale

ballast as its size disparity ratio R_D = 2.8 is greater than 2.4. However, in dense conditions segregation is less likely to occur, as R_D < 6.5. Nevertheless, R_D may not fully describe the segregation potential of a mixture, which may also be influenced by factors such as vibrational acceleration (Nakai and Yoshii, 2024). For example, Fiske *et al.* (1994) reported segregation in a mixture of perfect spheres with R_D = 4, when vibrated on a sieve shaker with a frequency and amplitude of 7.5 Hz and 1.5 cm, respectively.

Table 1. Summary of packing test results for the 1/3-scale ballast and the mixtures (M) with CR 0.8/3 and CR 3/7 with V_{cr}/V_a=10% and W_{cr}/W_a=10%, including crumb rubber content threshold, $CR_{c,th}$, size disparity ratio (calculated using Equation 3), R_D and minimum and maximum bulk unit weight, respectively γ_{min} and γ_{max}.

Nomenclature		1/3-scale ballast	M CR 0.8/3 V_{cr}/V_a=10%	M CR 0.8/3 W_{cr}/W_a=10%	M CR 3/7 V_{cr}/V_a=10%	M CR 3/7 W_{cr}/W_a=10%
Constituent	1/3-scale ballast (% by mass)	100	95	90	95	90
	Crumb rubber (% by mass)	0	5	10	5	10
R_D		-	7.1		2.8	
Loose packing	Weight* (kg)	36.57	36.77	36.03	35.33	36.77
	SD weight (kg)	0.5508	0.9760	0.0003	0.0002	0.0002
	Volume* (m^3)	0.0282	0.0279	0.0280	0.0280	0.0278
	SD volume (m^3)	0.0004	0.0004	0.0002	0.0002	0.0002
	γ_{min}* (kN/m^3)	12.72	12.94	12.61	12.39	11.88
	SD γ_{min} (kN/m^3)	0.1110	0.0253	0.0899	0.0874	0.1453
	$CR_{c,th}$ (by mass)	-	0.33		0.38	
Dense packing	Weight* (kg)	39.46	40.05	39.23	38.58	37.31
	SD weight (kg)	0.0000	0.5605	0.1501	0.1587	0.1361
	Volume* (m^3)	0.0276	0.0278	0.0277	0.0277	0.0278
	SD volume (m^3)	0.0002	0.0003	0.0000	0.0002	0.0001
	γ_{max}* (kN/m^3)	14.01	14.12	13.87	13.67	13.15
	SD γ_{max} (kN/m^3)	0.0808	0.0644	0.0685	0.0350	0.0423
	$CR_{c,th}$ (by mass)	-	0.32		0.36	

* Average values for 3 tests; SD = standard deviation

For the mixtures (M) with CR 0.8/3, the crumb rubber particles are small enough to move between the void spaces within the stone aggregate skeleton. As the crumb rubber content, CR_c, is lower than the threshold value, $CR_{c,th}$, a packing in which crumb rubber particles enter the aggregate voids as filling components, without disrupting the granular packing significantly, would be expected (Figure 2a). Hence the bulk unit weight would be expected to increase.

For mixtures (M) with CR 3/7, crumb rubber particles are not sufficiently different in size to enter the inter-aggregate voids without disrupting the stone aggregate packing, hence would be expected to separate aggregate particles rather than fill aggregate voids (Figure 2b). As a result, a reduction in the bulk unit weight would be expected to occur because denser stones are displaced by less dense crumb rubber particles.

Figure 5 shows the variation (in percentage) of the minimum and maximum bulk unit weight and the average aggregate crumb rubber mixture (M) grain specific gravity, relative to $^1/_3$-scale ballast stones.

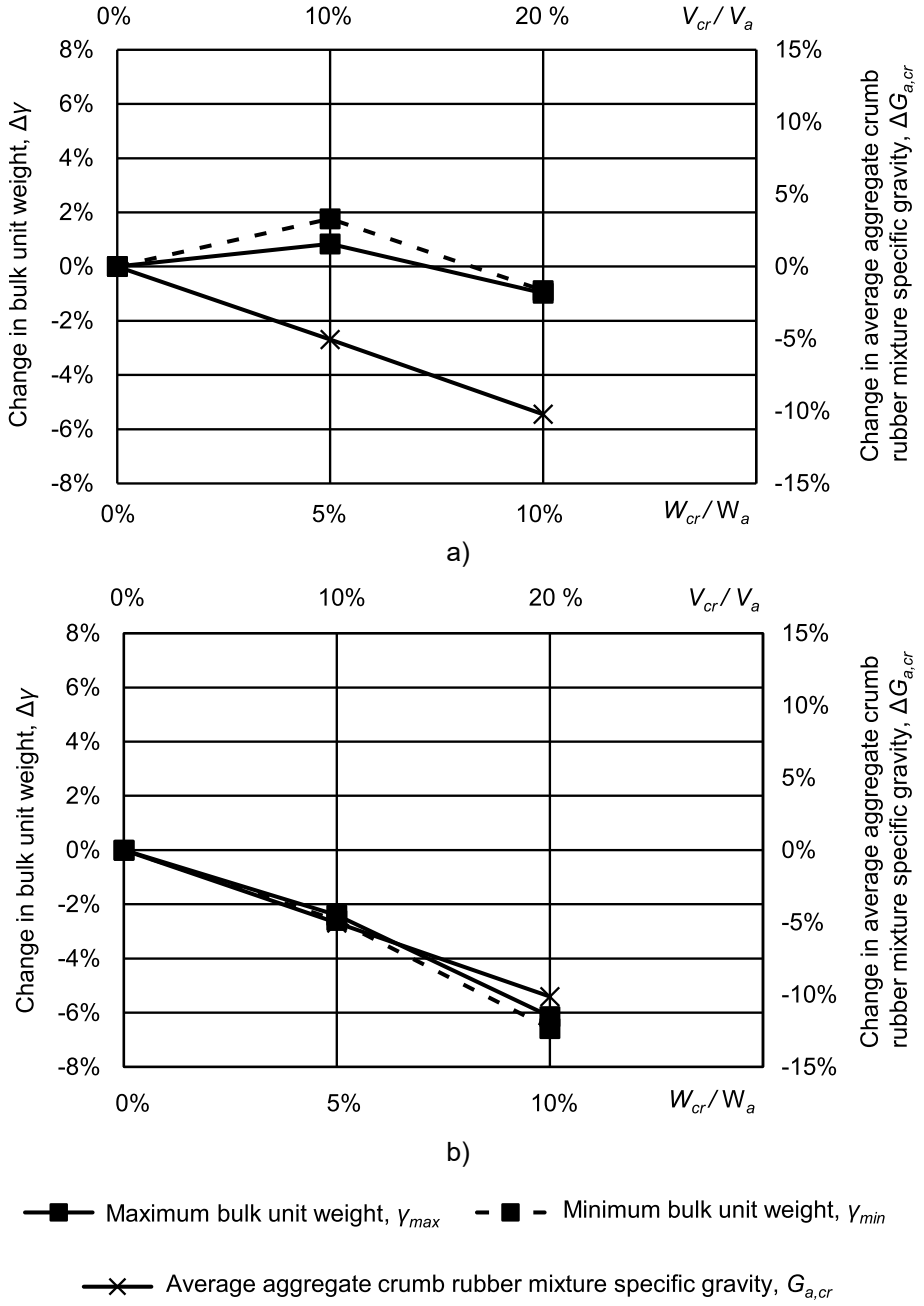

Figure 5. Variation (in percentage) of the minimum and maximum bulk unit weight and average aggregate crumb rubber mixture (M) specific gravity, relatively to the 1/3-scale ballast: a) CR 0.8/3 b) CR 3/7.

Relative to 1/3-scale ballast on its own, the addition of CR 0/8/3 crumb rubber initially (M CR 0.8/3 W_{cr}/W_a= 5%) caused an increase in the specimen bulk unit weight for both loose and dense packing (Table 1 and Figure 5). This is consistent with the crumb rubber filling the voids between the stone aggregate particles. However, the bulk unit weight then reduced for M

CR 0.8/3 W_{cr}/W_a=10%, which is still below the theoretical threshold level. This may have been because (i) the actual $CR_{c,th}$ is lower than that calculated by Equation 3, or (ii) the crumb rubber content may have deviated from the mixture target value (V_{cr}/V_a=10% or W_{cr}/W_a=10%), potentially exceeding $CR_{c,th}$, and / or (iii) the mix did not pack homogeneously.

The reduction in the bulk unit weight on adding crumb rubber CR 3/7 is consistent with these larger crumb rubber particles disrupting the aggregate skeleton, as would be expected.

Specimens were created by mixing a pre-determined mass of crumb rubber with 50 kg of $^1/_3$-scale ballast using a cement mixer. Alonso *et al.* (1991) reported that radial segregation occurs when two dry granular materials are mixed in a drum mixer operating in the cascade regime. In this regime, a thin surface layer of particles rolls down the slope that forms during rotation. The surface layer may sink into the underlying layers, leading to segregation (Ottino and Khakhar, 2000). In this experimental programme, when mixing crumb rubber with $^1/_3$-scale ballast in the cement mixer, radial segregation led to the formation of a core composed of crumb rubber particles (Figure 6). Mixed particles where then placed inside the test box (as described in section 2.3), with no additional steps taken to mitigate potential segregation.

Figure 6. Core of crumb rubber particles after using cement mixer.

This suggests that the content of crumb rubber in individual specimens may have deviated from the desired proportions. However, the maximum content of crumb rubber mixed with 50 kg of $^1/_3$-scale ballast was 5 kg for M CR 0.8/3 W_{cr}/W_a=10%. Even in the extreme (unlikely) case that all of the CR 0.8/3 in the cement mixer was transferred to the specimen box, the resulting dense packing mixture would contain approximately 13% of crumb rubber by weight, which is still well below the theoretical threshold of W_{cr}/W_a=32%.

The crumb rubber content threshold, $CR_{c,th}$ (Equation 3) was conceptualized for binary mixtures of readily-differentiable, incompressible particles. Figure 4 shows that crumb rubber particles exhibit considerable compressible and elastic deformation when sheared. At the micro-level, such deformability may inhibit efficient packing within a skeleton of rigid aggregate particles. This suggests either that the real $CR_{c,th}$ is lower than the theoretical value, or that the mixtures exhibit non-homogeneous packing (Figure 2c).

While filling Box 1, no obvious particle segregation or stratification was observed (from the top

of the box). However, some images of Box 2 after filling showed levels of crumb rubber segregation and stratification along the box height (Figure 7). This is consistent with the findings of Makse *et al.* (1997) as the $^1/_3$-scale ballast has a higher angle of response than crumb rubber. Under cyclic loading the degree of segregation increased, with a downward movement of crumb rubber (Figure 7; the red circle shows the segregation of crumb rubber within the aggregate matrix under cyclic loading). Segregation was perhaps more evident for the smaller crumb rubber, CR 0.8/3, than for the larger CR 3/7, consistent with the ability of smaller particles to ravel downward through the larger aggregate particle voids.

The observed layered packing is consistent with the monotonic triaxial test results reported by Qi *et al.* (2024) on ballast (D_{50} = 39 mm) intermixed with crumb rubber (9.5 mm to 19 mm), with crumb rubber contents W_{cr}/W_a = 5%,10% and 15% and R_D approximately 2 or 4. All specimens reported by Qi *et al.* (2024) showed reduced stiffness and reduced maximum deviatoric stress compared with the aggregate on its own, reflecting the disruption of ballast skeleton caused by the presence of crumb rubber particles, even for the lowest crumb rubber content tested, for more similarly-sized mixtures with R_D values below the limit for ready differentiation of the two fractions.

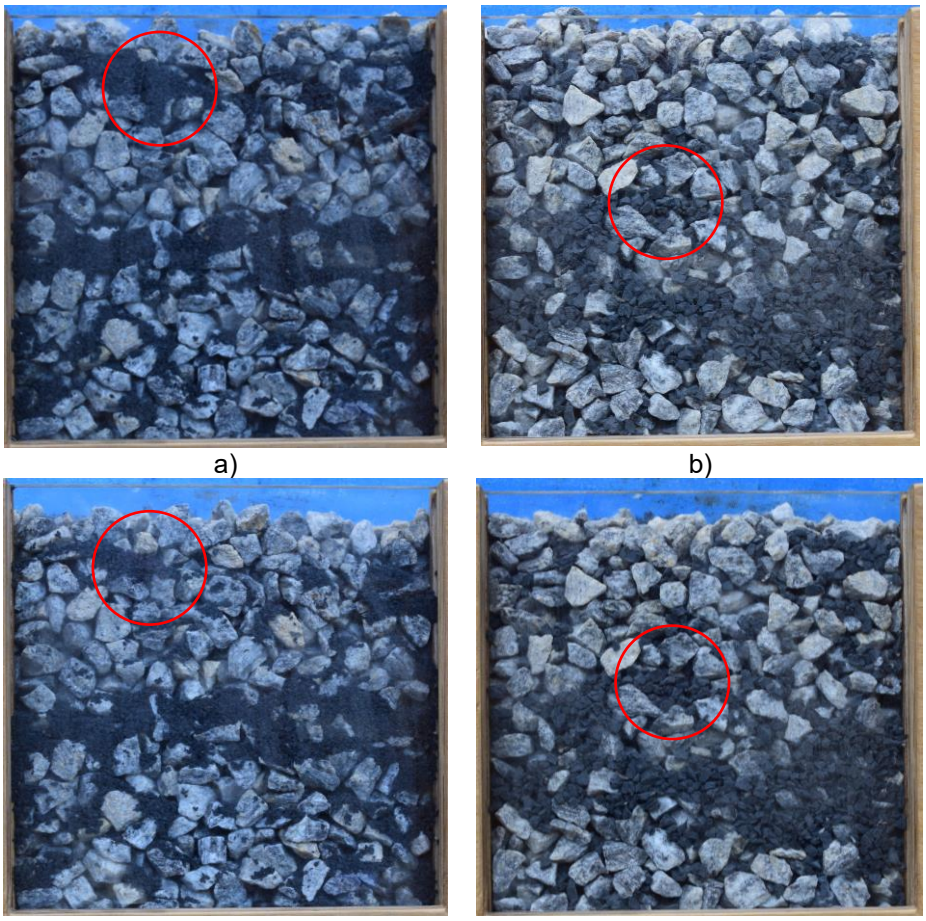

Figure 7. Crumb rubber stratification after being poured onto the box and segregation during compaction, highlighted by a red circle; a) M CR 0.8/3 W_{cr}/W_a = 10% before compaction, b) M CR 3/7 W_{cr}/W_a = 10% before compaction, c) M CR 0.8/3 W_{cr}/W_a = 10% after compaction, d) M CR 3/7 W_{cr}/W_a = 10% after compaction.

Given that mixtures may exhibit non-homogenous packing, an analysis of the packing using both the traditional two-phase framework and the proposed three-phase framework was carried out, assuming no segregation. The objective was to demonstrate how analytical results may, in certain cases, lead to misleading or erroneous conclusions. Table 2 presents the corresponding maximum and minimum void ratios, calculated using both the conventional two-phase framework (Equation 5, e_{global}) and the proposed three-phase framework (Equations 4 and 5). Figure 8 shows the variation (in percentage) of the minimum and maximum void ratios and the average aggregate crumb rubber mixture (M) specific gravity, relative to the $^1/_3$-scale ballast.

Table 2. Summary of packing test results expressed as the average aggregate crumb rubber mixture (M) specific gravity, $G_{a,cr}$, and maximum and minimum void ratio (e_{max} and e_{min}, respectively) obtained using the conventional two-phase framework (Equation 4) using $G_{a,cr}$ (Equation 1) to calculate the total volume of solid particles (aggregate plus crumb rubber) and the proposed three-phase framework (Equations 4 and 5)

Nomenclature		$^1/_3$-scale ballast	M CR 0.8/3 V_{cr}/V_a=10%	M CR 0.8/3 W_{cr}/W_a=10%	M CR 3/7 V_{cr}/V_a=10%	M CR 3/7 W_{cr}/W_a=10%
Two-phase framework (Equation 1)	$G_{a,cr}$ (-)	2.50	2.38	2.25	2.38	2.25
	e_{max} (-)	0.93	0.80	0.75	0.88	0.86
	SD e_{max} (-)	0.0168	0.0035	0.0125	0.0133	0.0229
	e_{min} (-)	0.75	0.65	0.59	0.71	0.68
	SD e_{min} (-)	0.0101	0.0075	0.0078	0.0044	0.0054
Three-phase framework (Equations 4 and 5)	$e_{intergran,max}$ (-)	0.93	1.00	1.17	1.09	1.30
	SD $e_{intergran,max}$ (-)	0.0168	0.0039	0.0155	0.0148	0.0283
	$e_{global,max}$ (-)	0.93	0.81	0.75	0.89	0.86
	SD $e_{global,max}$ (-)	0.0168	0.0035	0.0125	0.0134	0.0229
	$e_{intergran,min}$ (-)	0.75	0.83	0.97	0.89	1.08
	SD $e_{intergran,min}$ (-)	0.0101	0.0083	0.0097	0.0048	0.0067
	$e_{global,min}$ (-)	0.75	0.66	0.59	0.71	0.68
	SD $e_{global,min}$ (-)	0.0101	0.0075	0.0078	0.0044	0.0054

In the two-phase framework analysis (Table 2), the inclusion of crumb rubber led to a reduction in both the maximum (e_{max}) and minimum (e_{min}) void ratios of the mixtures (Figure 8). In contrast, the three-phase framework analysis (Table 2), and assuming that each specimen contained the desired crumb rubber content (Table 1), the inclusion of crumb rubber led to an increase in the intergranular void ratio, $e_{intergran}$, and a decrease in the global void ratio, e_{global}, for both loose and dense states (Figure 8). The global void ratios obtained for loose and dense packing (three-phase framework) are by definition the same as for the two-phase framework (minor differences are due to rounding). The maximum and minimum intergranular void ratios for the mixtures were larger than the corresponding values for $^1/_3$-scale ballast alone (Table 2, Figure 8). The observed increase in the intergranular void ratio is consistent with the crumb rubber starting to disrupt aggregate packing as in Figure 7, in every case.

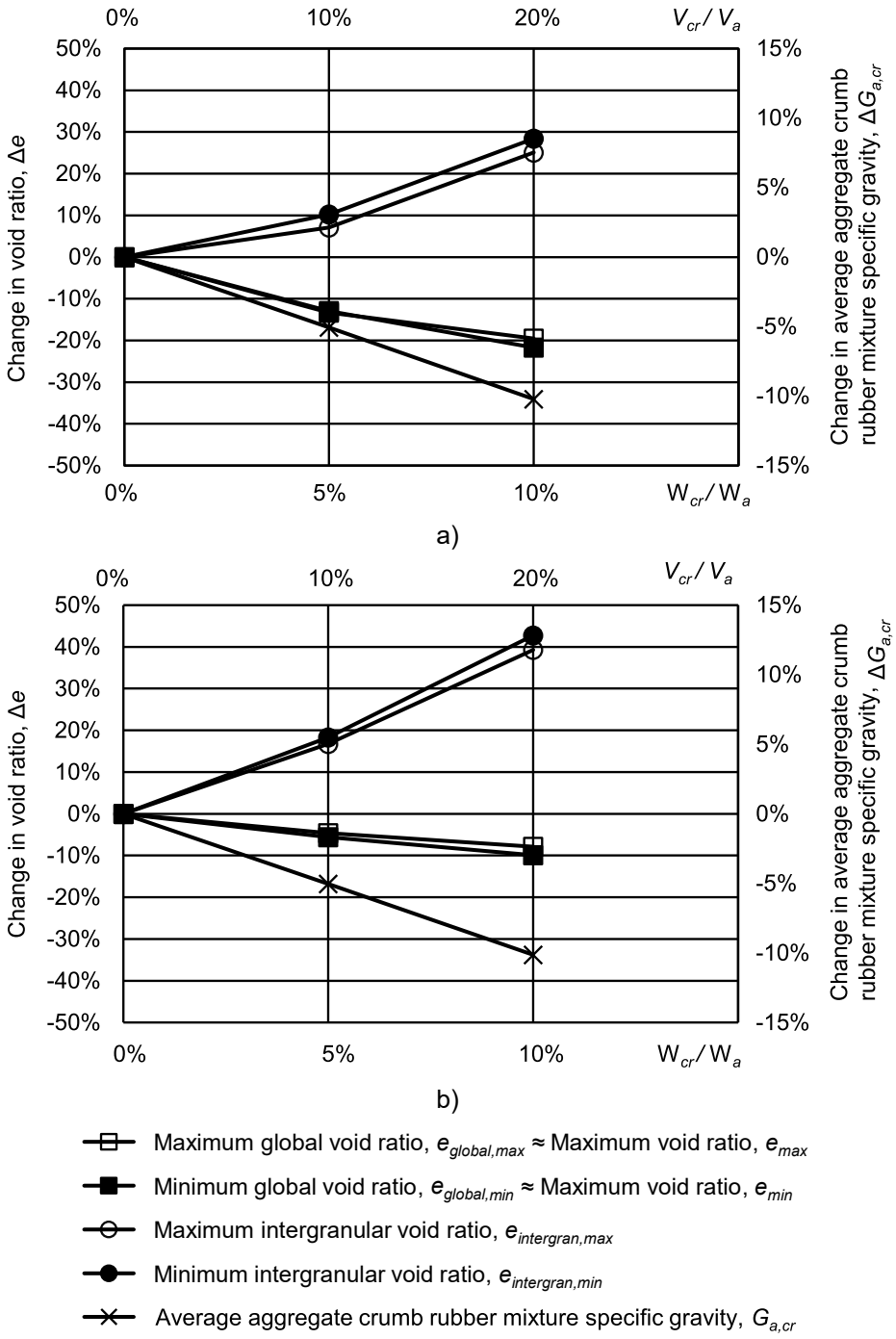

459 Figure 8. Variation (in percentage) of the minimum and maximum void ratios and the average
460 aggregate crumb rubber mixture (M) specific gravity, relatively to the $^1/_3$-scale ballast:
461 a) CR 0.8/3, b) CR 3/7.
462
463 The segregation and stratification phenomena need to be further explored as, if confirmed, the
464 potential benefits of adding crumb rubber to railway ballast reported in the literature may

diminish under cyclic loading and with time. Stratification (Figure 7) could diminish the benefits of reduced particle abrasion, possibly militating against the addition of crumb rubber to railway ballast. Furthermore, considering the crumb rubber as part of the solid phase, as in the two-phase framework, ignores the compressibility and lower density of the crumb rubber grains. A more accurate impression of the effect of adding crumb rubber is given by the change in the intergranular void ratio - which may increase, implying a reduction in density - than by the global void ratio, which always decreases.

4 Conclusions

In this paper, the effect of adding crumb rubber on the packing of a coarse aggregate was investigated. Packing tests in a box with transparent side windows enabled a visual assessment of particle packing, and any changes associated with the addition of crumb rubber, to be made. A framework to analyse the packing of aggregate crumb rubber mixtures has been proposed. The main conclusions of this work are:

1. The optimum crumb rubber content is commonly reported in the literature as 10%, but sometimes by weight and sometimes by volume. These are not the same, with 10% by weight of aggregate particles being nearly twice the mass of crumb rubber as 10% by volume of aggregate particles.

2. The crumb rubber material studied, when tested on its own in direct shear, exhibited strain hardening with no clear asymptote to the maximum shear stress. The response was significantly influenced by the elastic deformation of the rubber particles.

3. The addition of crumb rubber particles disrupted the natural packing of the $^1/_3$-scale ballast aggregates, even at proportions below the theoretical threshold for crumb rubber particles small enough to fit within the stone aggregate voids ($R_D > 6.4$). This is not altogether surprising, as the theoretical threshold is based on highly idealised conditions and the actual content of crumb rubber for each specimen may have deviated from the desired value.

4. Treating the crumb rubber as a third phase, separate from either the voids or the aggregates, leads to a more realistic and useful description of the packing of crumb rubber-aggregate

mixtures than a more traditional two-phase approach in which both the crumb rubber and the stone aggregates are lumped together as solids.

5. In the cement mixer used to mix aggregates and crumb rubber particles, radial segregation can result in the formation of a core composed almost entirely of crumb rubber particles. When operating in the cascade regime, a cement mixer might not be the ideal solution to mix two dry granular materials of different particle density and / or particle size.

6. Segregation and stratification of crumb rubber was observed when pouring the mixtures into the clear-sided test box, for both of the crumb rubber size tested. Smaller rubber particles, CR 0.8/3, appeared to be more susceptible to segregation (by ravelling) than larger ones, CR 3/7, as they were small enough to pass between the stone intergranular voids. The degree of segregation increased under applied cyclic loading. This might have implications for the large-scale application of crumb rubber addition in railway ballast.

7. Mixing methods and segregation mechanisms need further study. Future work could include representative tests (for example, monotonic and cyclic triaxial tests) on full size materials. Conducting and interpreting these in the light of the framework proposed in this paper could enable a better understanding of the mechanics governing the interaction of elastic granular materials mixed with stone aggregates.

Acknowledgements

This research was supported by the doctoral Grant PRT/BD/154385/2022 and DOI identifier 10.54499/PRT/BD/154385/2022 financed by Portuguese Foundation for Science and Technology (FCT), and with fund from the State Budget, from the European Social Fund (ESF) made available under Regional Operational Program of the Centre (Centro 2020), under MIT Portugal Program. This research was funded in whole or in part by the Fundação para a Ciência e a Tecnologia, I.P. (FCT, https://ror.org/00snfqn58) under Grant UID/6438/2025 of the research unit CERIS. For the purpose of Open Access, the author has applied a CC-BY public copyright license to any Author's Accepted Manuscript (AAM) version arising from this submission.

The Authors also acknowledge the supply of crumb rubber by *Genan* (Aveiro, Portugal).

CENTRO2020 REPÚBLICA PORTUGUESA EDUCAÇÃO, CIÊNCIA E INOVAÇÃO UNIÃO EUROPEIA Fundo Social Europeu fct Fundação para a Ciência e a Tecnologia MIT Portugal

References

Ahmed, I. and Lovell, C.W. (1993), "Rubber soils as lightweight geomaterials", *Transportation Research Record,* No.1422, pp. 61–70.

Aingaran, S. (2014), "Experimental investigation of static and cyclic behaviour of scaled railway ballast and the effect of stress reversal", University of Southampton, Faculty of Engineering and the Environment Civil and Environmental Engineering, PhD thesis, p.161.

Ajayi, O. (2014), "The Effect of Fibre Reinforcements on the Mechanical Behaviour of Railway Ballast, University of Southampton, Faculty of Engineering and Physical Sciences Civil and Environmental Engineering, PhD thesis, pp.69.

Alonso, M. Satoh, M. and Miyanami, K. (1991), "Optimum combination of size ratio, density ratio and concentration to minimize free surface segregation", *Powder Technology*, Vol. 68 No. 2 ,pp.145-152, doi.org/10.1016/0032-5910(91)80122-Y.

Arachchige, C.M.K. Indraratna, B. Qi, Y. Vinod, J.S. and Rujikiatkamjorn, C. (2022), "Deformation and degradation behaviour of Rubber Intermixed Ballast System under cyclic loading", *Engineering Geology*, Vol 307,doi.org/10.1016/j.enggeo.2022.106786.

Arachchige, C.M.K. Indraratna, B. Qi, Y. Vinod, J.S. and Rujikiatkamjorn, C. (2021),"Geotechnical characteristics of a Rubber Intermixed Ballast System", *Acta Geotechnica*, Vol 17, pp.1847–1858. doi:10.1007/s11440-021-01342-2.

British Standards Institution, (2012),"Aggregates for railway ballast", BSI London, United Kingdom.

British Standards Institution (2022), "Tests for mechanical and physical properties of aggregates - Determination of particle density and water absorption". BSI London, United Kingdom.

Brown, S,F. Kwan, J. and Thom, N.H. (2007), "Identifying the key parameters that influence geogrid reinforcement of railway ballast", *Geotextiles and Geomembranes* Vol. 25 No. 6, pp.326–335, doi:10.1016/j.geotexmem.2007.06.003.

D'Angelo, G. Thom, N. and Lo Presti, D. (2016), "Bitumen stabilized ballast: A potential solution for railway track-bed", *Construction and Building Materials*, Vol.124, pp.118–126, doi:10.1016/j.conbuildmat.2016.07.067.

De Andrade, M.S.F.G. and Dieguez, A.C. Delgado G.B. and Lima, T.B. and Guimarães, R.C.A. (2025), " Mechanical behaviour of limestone ballast for heavy haul Brazilian railway lines: Laboratory evaluation", Transportation Geotechnics, Vol.52, https://doi.org/10.1016/j.trgeo.2025.101547.

Delgado, G.B. and Fonseca, A.V. and Fortunato, E. and Maia, P. (2019), " Mechanical behaviour of inert steel slag ballast for heavy haul rail track: Laboratory evaluation", Transportation Geotechnics, Vol. 20, https://doi.org/10.1016/j.trgeo.2019.100243.

Dunn, S. and Bora P.K. (1972), "Shear strength of untreated road base aggregates measured by variable lateral pressure cell", *Journal of Materials*, Vol.7 No.2, pp.131-142.

Edil, T.B. (1988), "Soil fabric", *General Geology*. Encyclopedia of Earth Science, pp.778–788, doi:10.1007/0-387-30844-X_105.

Esmaeili, M. Paricheh, M. and Esfahani, M.H. (2020), "Laboratory investigation on the behavior of ballast stabilized with bitumen-cement mortar", *Construction and Building Materials*, Vol.245, doi:10.1016/j.conbuildmat.2020.118389.

Esmaeili, M. Zakeri, J.A. Ebrahimi, K.S. and Sameni, M.K. (2016), “Experimental study on dynamic properties of railway ballast mixed with tire derived aggregate by modal shaker test”, *Advances in Mechanical Engineering*. Vol.8 No.5, , doi:10.1177/1687814016640245.
Esveld, C. (2003), *Recent developments in slab track*. In European Railway Review, Russell Publishing LTD, Kent, UK.
Ferro, E. Le Pen, L. Zervos, A. and Powrie, W. (2024), “Fibre-reinforcement of railway ballast to reduce track settlement”, *Geotechnique*, Vol.74 No.9, pp.862-874, doi:10.1680/jgeot.21.00421.
Fiske, T.J. Railkar, S.B. and Kalyon, D.M. (1994), “Effects of segregation on the packing of spherical and nonspherical particles” *Powder Technology*, Vol.81 No.1, pp.57-64, https://doi.org/10.1016/0032-5910(94)02862-1.
Guo, Y. Markine, V. Qiang, W. Zhang, H and Jing, G. (2019), “Effects of crumb rubber size and percentage on degradation reduction of railway ballast” *Construction and Building Materials*,Vol.212, pp.210–224, doi:10.1016/j.conbuildmat.2019.03.315.
Gupta, A. (2023), “Mechanical Properties of Re-used Ballast”, University of Southampton, Faculty of Engineering and Physical Sciences Civil and Environmental Engineering, PhD thesis, pp.86-89.
Indraratna, B. and Khabbaz, H. and Salim, W. and Christie. D (2006), “Geotechnical properties of ballast and the role of geosynthetics in rail stabilisation”, *Ground Improvement*, Vol. 10 No.3, pp. 91-101. https://doi.org/10.1680/grim.2006.10.3.91
Indraratna, B. (2023), “*Effective and eco-friendly solutions for Australia’s railways”*, available at: https://atse.org.au/news/effective-and-eco-friendly-solutions-for-australias-railways/ (accessed: 4 February 2025)
Kennedy, J. Woodward, P.K. Medero, G. and Banimahd, M. (2013), “Reducing railway track settlement using three-dimensional polyurethane polymer reinforcement of the ballast” *Construction and Building Materials*, Vol.44, pp.615–625, doi:10.1016/j.conbuildmat.2013.03.002.
Kirkpatrick, W.M. (1965), “Effects of grain size and grading on the shear behaviour of granular material”, In: Proc 6th International Conference on Soil Mechanics and Foundation Engineering, Montréal; pp.273-277.
Koike, Y. and Nakamura, T. and Hayano K. and Momoya, Y. (2014), “Numerical method for evaluating the lateral resistance of sleepers in ballasted tracks”, *Soils and Foundation*, Vol. 54 No.3, pp. 502-514,https://doi.org/10.1016/j.sandf.2014.04.014.
Koohmishi, M. and Azarhoosh, A. (2021), “Degradation of crumb rubber modified railway ballast under impact loading considering aggregate gradation and rubber size”, *Canadian Geotechnical Journal*, Vol.58 No.3, pp.398–410, doi:10.1139/cgj-2019-0596.
Kudrolli, A. (2004), “Size separation in vibrated granular matter” *Reports on Progress in Physics*, Vol.67 No.3,pp.209–247, doi:10.1088/0034-4885/67/3/R01.
Lade, P.V. (2016), *Triaxial Testing of Soils*, John Wiley & Sons, London, UK.
Le, T.H.M. Lee, S.H. and Park, D.W. (2020), “Evaluation on full-scale testbed performance of cement asphalt mortar for ballasted track stabilization” *Construction and Building Materials*, Vol.254, doi:10.1016/j.conbuildmat.2020.119249.
Le Pen, L.M. Powrie, W. Zervos, A. Ahmed, S. and Aingaran, S. (2013), “Dependence of shape on particle size for a crushed rock railway ballast”, *Granular Matter*, Vol.15 No.6, pp.849–861, doi:10.1007/s10035-013-0437-5.
Le Pen, L. and Bhandari, A.R. and Powrie, W. (2014), “ Sleeper End Resistance of Ballasted Railway Tracks”, *Journal of Geotechnical and Geoenviromental Engineering*, Vol. 140 No.5, https://doi.org/10.1061/(ASCE)GT.1943-5606.0001088
Lee, J.S. Dodds, J. and Santamarina, J.C. (2007), “Behavior of Rigid-Soft Particle Mixtures” *Journal of Materials in Civil Engineering*, Vol.19 No.2, pp.179–184, doi:10.1061/ASCE0899-1561200719:2179.

Leslie, D.D. (1963), “Large-scale triaxial tests on gravely soils”, In: Proc. 2nd Pan American Conference on Soil Mechanics and Foundations Engineering, São Paulo, Brazil, pp.181-202.
Liang, W. Wu, M. Liu, F. Zheng, K. and He, J. (2025), “Small-strain dynamic characteristics of multilayered rubber-sand composites” *Geosynthetics International*. doi:10.1680/jgein.24.00140.
Makse, H.A Havlin, S. King, P.R. and Stanley, H.E. (1997), “Spontaneous stratification in granular mixtures”, *Nature*, Vol.386, pp.379–382, doi:10.1038/386379a0.
Mitchell, J. Soga, K. and O´Sullivan, C. (2025), *Fundamentals of Soil Behavior*, 4th edition,. Wiley.
Nakai, F. and Yoshii, k. (2024), “Reducing segregation in vibrated binary-sized granular mixtures by excessive small particle introduction” *Granular Matter*, Vol.27 , doi.org/10.1007/s10035-024-01476-6
Ottino, J.M. and Khakhar, D.V. (2000), “Mixing and Segregation of Granular Materials” *Annual Review of Fluid Mechanics*,Vol.32, pp.55-91, doi.org/10.1146/annurev.fluid.32.1.55
Qi, Y., Indraratna, B., Ngo, T., Arachchige, C.M.K. and Hettiyahandi, S. (2024), “Sustainable solutions for railway using recycled rubber”, *Transportation Geotechnics*,Vol.46. doi:10.1016/j.trgeo.2024.101256.
Rempelos, G. Ortega, A. Blainey, S. Preston, J. Le Pen, L. and Armstrong, J. (2020), “A method for assessing the life cycle costs of modifications to ballasted track systems”, *Construction and Building Materials*. Vol. 263, doi:10.1016/J.CONBUILDMAT.2020.120603.
Rosato, A. Strandburg, K.S. Prinz, F. and Swendsen, R.H. (1987), “Why the Brazil Nuts Are on Top: Size Segregation of Particulate Matter by Shaking”, *Physical Review Letters*, Vol.58, pp.1038–1040, doi.org/10.1103/PhysRevLett.58.1038
Selig, E.T. and Roner, C.J. (1987), “Effect of particle characteristics on behaviour of granular materials”, *Transportation Research record* , Transportation Research board, National Research Council, Washington DC.
Sevi, A.F. (2008), “*Physical modeling of railroad ballast using the parallel gradation scaling technique within the cyclical triaxial framework”,* Missouri University of Science and Technology, PhD thesis.
Shenton, M.J. (1978), “Deformation of railroad ballast under repeated load conditions” *Railroad Track Mechanics and Technology*, In. Proceedings of a Symposium held at Princeton University pp.405-425, doi.org/10.1016/B978-0-08-021923-3.50025-5
Sol-Sánchez, M. Thom, N.H. Moreno-Navarro, F. Rubio-Gámez, M.C. and Airey, G.D. (2015), “A study into the use of crumb rubber in railway ballast” *Construction and Building Materials*, Vol.75, pp.19–24, doi:10.1016/j.conbuildmat.2014.10.045.
Suiker. A.S.J. Seling, E.T. and Frenkel, F. (2005), “Static and Cyclic Triaxial Testing of Ballast and Subballast”, *Journal of Geotechnical and Geoenviromental Engineering*, Vol. 131 No.6, pp.771-782, https://doi.org/ 10.1061/(ASCE)1090-0241(2005)131:6(771)
Tasalloti, A. Chiaro, G. Murali, A. and Banasiak, L. (2021), “Physical and mechanical properties of granulated rubber mixed with granular soils—a literature review” *Sustainability,*Vol.13 No.8. doi:10.3390/su13084309.
Thevanayagam, S. Shenthan, T. Mohan, S. and Liang, J. (2002), “Undrained Fragility of Clean Sands, Silty Sands, and Sandy Silts”, Journal of Geotechnical and Geoenviromental Engineering,Vol. 128, No.10, doi:10.1061/ASCE1090-02412002128:10849.
Vallerga, B.A. Seed, H.B. Monismith, C.L. and Cooper, R.S. (1956), “Effect of shape, size and surface roughness of aggregate particles on the strength of granular materials”, Advancing Standards Transforming Markets, pp. 63-76.
Xiao, M. Ledezma, M. and Hartman, C. (2015), “Shear Resistance of Tire-Derived Aggregate Using Large-Scale Direct Shear Tests”, *Journal of Materials in Civil Engineering*, Vol.27 No.1,. doi:10.1061/(asce)mt.1943-5533.0001007.

Xu, C. and Nakamura, T. and Murakami, T. and Hayano, K. (2024), “Development of a scaled model test method for a dynamic and continuous survey to detect variations in the lateral stability of ballasted tracks”, *Transportation Geotechnics*, Vol 45, https://doi.org/10.1016/j.trgeo.2024.101198.

Figure captions (images as individual files separate to your MS Word text file).

Figure 1. Particle size distribution of the 1/3-scale ballast , the corresponding full-scale ballast (within the BS EN 13450 limits) and the two crumb rubber ranges (CR 0.8/3 and CR 3/7).

Figure 2. Role of crumb rubber within aggregate packing for $CR_c < CR_{c,th}$ (simplified and incompressible particle shapes: spheres): a) Confined within aggregate particles [crumb rubber does not take part in the load path],b) Confined and partly in contact with aggregate particles [crumb rubber particles take some part in the load path], c) Layered [load path alternates through the aggregates and the crumb rubber with depth].

Figure 3. Assemblage of spheres in regular packing (adapted from Mitchell *et al.*, 2025).

Figure 4. Crumb rubber direct shear test results (shear stress ,τ, plot against shear strain, δ) for different normal stresses a) CR 0.8/3 b) CR 3/7.

Figure 5. Variation (in percentage) of the minimum and maximum bulk unit weight and average aggregate crumb rubber mixture (M) specific gravity, relatively to the 1/3-scale ballast: a) CR 0.8/3 b) CR 3/7.

Figure 6. Core of crumb rubber particles after using cement mixer.

Figure 7. Crumb rubber stratification after being poured onto the box and segregation during compaction, highlighted by a red circle; a) M CR 0.8/3 Wcr/Wa = 10% before compaction, b) M CR 3/7 Wcr/Wa = 10% before compaction, c) M CR 0.8/3 Wcr/Wa = 10% after compaction, d) M CR 3/7 Wcr/Wa = 10% after compaction.

Figure 8. Variation (in percentage) of the minimum and maximum void ratios and the average aggregate crumb rubber mixture (M) specific gravity, relatively to the 1/3-scale ballast: a) CR 0.8/3, b) CR 3/7.

Editor’s note: do not copy and paste your images into MS Word, this reduces their quality. Instead upload them to the journal website as separate files in the format used to originally create them.